Cooperative Spectrum Sensing in TV White Space Scenarios with Fading and Impulsive Noise

André A. Anjos*, Diogo C. Arvelos*, Luís M. A. Borges*, Yonghui Li‡, and Rausley A. A. de Souza†‡
*Universidade Federal de Uberlândia (UFU), Patos de Minas, MG, Brazil
†National Institute of Telecommunications, Inatel, Santa Rita do Sapucaí, MG, Brazil
‡University of Sydney, Sydney, NSW, Australia
Email: {andre.anjos,diogo.arvelos,luis.alves}@ufu.br, yonghui.li@sydney.edu.au, rausley@inatel.br

***Abstract*—This paper evaluates the performance of cooperative spectrum sensing in TV White Spaces (TVWS) environments under impulsive noise using sample and decision fusion methods employing the majority rule. Realistic scenarios are considered with orthogonal frequency division multiplexing (OFDM) signals transmitted in the ISDB-T/TB TV standard, used in several countries, including Japan, Brazil, and others. We investigate the performance of the cooperative energy detection technique under various conditions, including additive white Gaussian noise, multipath fading, and impulsive noise. The results demonstrate that cooperative sensing can significantly improve detection probability and reduce false alarm rates compared to non-cooperative ones. The study highlights the impact of impulsive noise on system performance. It emphasizes the importance of choosing the correct decision rule in enhancing the reliability of spectrum sensing in cognitive radio networks. It also considers the number of radios in the cooperative network and the number of samples collected by each cognitive radio, among other factors. The findings contribute to developing more efficient spectrum utilization strategies for wireless communication systems in TVWS, helping solve the spectrum scarcity problem.**

***Index Terms*—TV White Spaces, cooperative spectrum sensing, impulsive noise, energy detection, ISDB-T$_B$, OFDM.**

I. Introduction

The frequency spectrum is a valuable resource in the area of wireless communication. However, only a small portion can be used due to technical and political limitations, making it scarce and expensive. Analyses by different authors around the world have shown that the current spectrum scarcity scenario arises not only from a physical limitation of the electromagnetic spectrum but also from its underutilization [1], largely due to the current fixed spectrum allocation policy, which becomes more evident in the VHF (very high frequency) and UHF (ultra high frequency) bands, which are intended for TV channel allocation.

This work was partially supported by Minas Gerais Research Foundation (FAPEMIG) (RED-00194-23), under Minas Gerais Research Network in 5G and 6G project, by Rede Nacional de Ensino e Pesquisa (RNP), with resources from Ministério da Ciência, Tecnologia e Inovações (MCTIC), under the Brazil 6G Project of the Radiocommunication Reference Center (Centro de Referência em Radiocomunicações (CRR)) of the National Institute of Telecommunications (Instituto Nacional de Telecomunicações (Inatel)), Brazil, under Grant 01245.010604/2020-14, by CNPq (Grant References 311470/2021-1 and 403827/2021-3), by the projects XGM-AFCCT-2024-2-5-1 and XGM-FCRH-2024-2-1-1 supported by xGMobile – EMBRAPII-Inatel Competence Center on 5G and 6G Networks, with financial resources from the PPI IoT/Manufatura 4.0 from MCTI grant number 052/2023, signed with EMBRAPII, and by Fapemig (PPE-00124-23).

The unused spaces of the TV spectrum have become known worldwide as TV White Spaces (TVWS). They are emerging, along with a new policy of dynamic spectrum allocation called dynamic spectrum access (DSA), as a solution to overcome this problem of "scarcity" and make spectrum use more efficient. Recently, the National Telecommunications Agency (ANATEL) board of directors in Brazil approved a proposal to regulate the dynamic use of idle TVWS spectrum by secondary users [2]. The approved resolution proposal assigns and designates VHF and UHF bands for this type of application, initially considering the 54-72 MHz, 174-216 MHz, 470-608 MHz, and 614-698 MHz bands. "*The regulations regulate the application of this technology, which allows the dynamic designation of radio frequencies intended for broadcasting that are not authorized for telecommunications services. This dynamic use of idle TVWS spectrum increases the efficiency of using spectrum, a limited resource, with characteristic advantages of TV frequency bands, such as long-range and tolerance to obstacles*" [2]. Thus, to utilize this resource efficiently, it is necessary to study and develop increasingly intelligent radios equipped with new technologies. These intelligent radios are called cognitive radios (CRs) [3] and promise to solve the problem of electromagnetic spectrum scarcity by their main functionality, namely spectrum sensing (SS).

In non-cooperative SS (non-CSS), each CR performs spectrum monitoring independently, without sharing information with other CRs, which may result in an unreliable decision. Another approach would be the cooperative SS (CSS), in which several CRs collect information from a channel, such as the received samples or individual decisions about occupancy, and send it to a fusion center (FC), which makes a global and more reliable decision about the channel's occupancy state.

Several studies in the field of SS address different scenarios and use different implementation techniques. For example, the authors in [4] present research on CR non-cooperative architectures and SS techniques such as matched filtering, energy detection (ED), and cyclostationary detection. However, non-CSS suffers greatly from decision inaccuracies due to practical problems such as receiver noise and multipath fading [5]. Authors in [6] present a study addressing CSS under imperfect reporting channels. Meanwhile, in [7], the problem of hidden nodes is presented as one of the most challenging issues in CSS, and the Graph Convolutional Networks (GCN)-CSS is

proposed, a cooperative spectral detection methodology based on GCN that adapts to dynamic changes in the CR network. However, despite the variety of scientific efforts, there is still a shortage of works focusing on more realistic disturbs and practical applications of SS techniques.

In this context, the present work aims to deepen the exploration of CSS in TVWS scenarios through MATLAB simulations, adopting a more realistic approach focusing on future practical implementation in software-defined radio. The study presented here offers the following contributions:

1) The primary user (PU) signal considered in the analyses is fully compliant with those encountered in practice in the TVWS bands in Japan, Brazil, and several other countries, specifically an OFDM signal with a 5.57 MHz bandwidth of the ISDB-T/$\mathrm{T_B}$ type;
2) A pessimistic TVWS sensing scenario with fading is also considered, where the CRs operate in a non-line-of-sight (nLoS) environment;
3) Beyond the additive white Gaussian noise (AWGN), we have also considered the impact of impulsive noise (IN) on the CSS performance for TVWS;
4) The performance of two distinct data fusion techniques in CSS, sample fusion (SF) and decision fusion (DF) methods, is evaluated in several TVWS scenarios, leading to interesting and novel conclusions regarding the conditions under which each method performs optimally.

The remainder of this article is structured as follows. Section II presents the mathematical modeling of the SS system, along with the impulsive noise model and the primary user signal considered in this work. Section III details the TVWS SS simulation setup. The results are discussed in Section IV. Finally, Section V offers concluding remarks.

II. System Model

A. Mathematical Modeling of a Spectrum Sensing System

The considered model consists of two hypotheses that will be used for decision-making, namely $\mathcal{H}_0$ and $\mathcal{H}_1$. The $\mathcal{H}_0$ hypothesis considers the absence of a PU signal in the sensed band, while the $\mathcal{H}_1$ hypothesis refers to the presence of a PU signal in that same band. The two hypotheses can be mathematically described as

$$y(t) = \begin{cases} w(t) + r(t), & \text{if } \mathcal{H}_0 \\ x(t)h(t) + w(t) + r(t), & \text{if } \mathcal{H}_1 \end{cases}, \tag{1}$$

where $y(t)$ is the signal captured and analyzed by the CR, $w(t)$ and $r(t)$ correspond to the thermal and impulsive noises in the receiver, respectively, $h(t)$ represents the gain or attenuation caused by the communication channel, and $x(t)$ is the PU transmitted signal. A decision variable, T_{ED}, generated by processing $y(t)$, must be defined to decide about spectral occupancy. This variable will depend on the sensing technique and a decision threshold, λ. Thus, if $T_{\mathrm{ED}} > \lambda$, it is decided that the spectrum is occupied; otherwise, it is considered free.

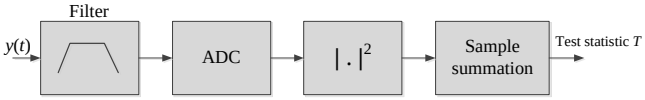

Figure 1. Simplified block diagram of the energy detection technique.

B. Energy Detection Technique

Several SS techniques are available, among which cyclostationary detection [8], matched-filter detection [9], and eigenvalue-based detection [10] can be cited. However, due to its low implementation complexity, ED is currently the most widely used technique [11], [12]. It is considered an optimal technique when no prior knowledge of the transmission signal is available and the thermal noise is not a source of uncertainty. In this technique, the detection of the presence or absence of the signal is based on monitoring the energy measured in the channel, compared to a decision threshold. Despite being a well-established sensing technique, nowadays, it still attracts considerable attention from researchers worldwide [13], [14]. Fig. 1 depicts a simplified block diagram for implementing the ED technique in the time domain. Following the block diagram shown in Fig. 1, a bandpass filter centered at the frequency of the channel of interest is first used. Subsequently, the filtered signal is down-converted to the baseband and digitized by an analog-to-digital converter (ADC), generating squared samples. The decision statistic, T_{ED}, is then calculated according to

$$T_{\mathrm{ED}} = \sum_{i=1}^{n} |y(i)|^2 , \tag{2}$$

where n is the total number of collected samples and $y(i)$ represents the i-th digitized sample collected by the CR. After the calculation of T_{ED}, its value is compared with λ for decision-making about which of the two hypotheses, $\mathcal{H}_0$ or $\mathcal{H}_1$, will be considered. Disregarding the IN, in the presence or absence of the primary signal, the decision variable has a chi-square distribution with n degrees of freedom [15]. Considering a sufficiently large number of samples, n, and using the central limit theorem, this variable can be approximated to a Gaussian random variable (RV), $T_{\mathrm{ED}} = \mathcal{N}(n\sigma_{\mathrm{w}}^2, n\sigma_{\mathrm{w}}^4)$ under hypothesis $\mathcal{H}_0$ and $T_{\mathrm{ED}} = \mathcal{N}(n(\sigma_{\mathrm{s}}^2+\sigma_{\mathrm{w}}^2), n(\sigma_{\mathrm{s}}^2+\sigma_{\mathrm{w}}^2)^2)$ under hypothesis $\mathcal{H}_1$, and thus, the average probabilities of false alarm and detection can be numerically found, respectively, as

$$P_{\mathrm{fa}} = Q\left(\frac{\lambda - n\sigma_{\mathrm{w}}^2}{\sqrt{n\sigma_{\mathrm{w}}^4}}\right), \tag{3}$$

$$P_{\mathrm{d}} = Q\left(\frac{\lambda - n(\sigma_{\mathrm{s}}^2+\sigma_{\mathrm{w}}^2)}{\sqrt{n(\sigma_{\mathrm{s}}^2+\sigma_{\mathrm{w}}^2)^2}}\right), \tag{4}$$

where σ_{w}^2 and σ_{s}^2 are the noise and PU signal variances, respectively and $Q(\cdot)$ is the Q-function, commonly used for solving problems involving numerical integration of area in Gaussian distributions.

Suppose the considered fading channel is of the Rayleigh type under slow fading, modeling a radio mobile environment

with nLoS. In that case, the signal-to-noise ratio (SNR) will vary randomly in each sensing period, exhibiting a statistical behavior described by an exponential probability density function as $f_\gamma(\gamma) = \frac{1}{\overline{\gamma}} e^{-\frac{\gamma}{\overline{\gamma}}}$, where γ and $\overline{\gamma}$ refer to the instantaneous and average SNRs, respectively. The average detection probability is given in its integral form by

$$P_{\mathrm{d}} = \int_0^\infty \frac{1}{\overline{\gamma}} e^{-\frac{\gamma}{\overline{\gamma}}} Q\left(\frac{\lambda - n\left(\overline{\gamma}+1\right)}{\sqrt{n\left(\overline{\gamma}+1\right)^2}}\right) \mathrm{d}\gamma. \tag{5}$$

To define the threshold to be used, a constant false alarm rate value is used, which can be calculated by isolating λ in (3), and then

$$\lambda = \sigma_{\mathrm{w}}^2 (Q^{-1}(P_{\mathrm{fa}})\sqrt{n} + n). \tag{6}$$

This work evaluates two approaches to the cooperative version of the ED technique. Firstly, the sample fusion (SF), in which all m CRs of the secondary network send their collected samples from the sensing channel to an FC, where they are used to compute a joint decision variable calculated in a similar way to that in (2), but using samples from all CRs, totaling $m \times n$ samples processed. Secondly, the majority-rule decision fusion (DF), in which each CR sends only its individual decision about the spectrum occupancy to an FC. The majority rule has been chosen for the analyses in this work because it provides a balanced approach. It provides greater robustness against individual sensor errors compared to the OR rule, reducing the probability of false positives while being less stringent than the AND rule, which allows for an increased probability of detection. If most decisions indicate that the spectrum is occupied, the FC decides it is occupied; otherwise, it is considered free.

CSS using SF is more complex to implement in practice since it would require transmitting the samples to the FC at a relatively high rate. On the other hand, the DF approach would only require sending a single bit indicating spectrum occupancy for each channel. The main idea of this work is to evaluate the performance differences and trade-offs between these two types of CSS under practical impairing conditions in TVWS scenarios.

C. Impulsive Noise Modeling

Impulsive noise, often caused by sources such as electrical switching, lightning, and engine ignition systems, can significantly degrade the performance of telecommunications and SS systems. It introduces high-amplitude disturbances that can interfere with signal detection and transmission. There are several models available in the literature for characterizing the IN. The IN model used in this work was proposed in [16]. This model assumes that the number of IN pulses within a given interval follows a Poisson distribution. The interval between occurrences can be modeled using an exponential distribution, given by $f(t) = \frac{1}{\beta} e^{-\frac{1}{\beta}t}$, where $t \geq 0$ is the time interval between consecutive pulses and β is the average time separation between them. Thus, without loss of generality, a random number with an exponential distribution of mean β samples is used to calculate the number of samples between two IN pulses.

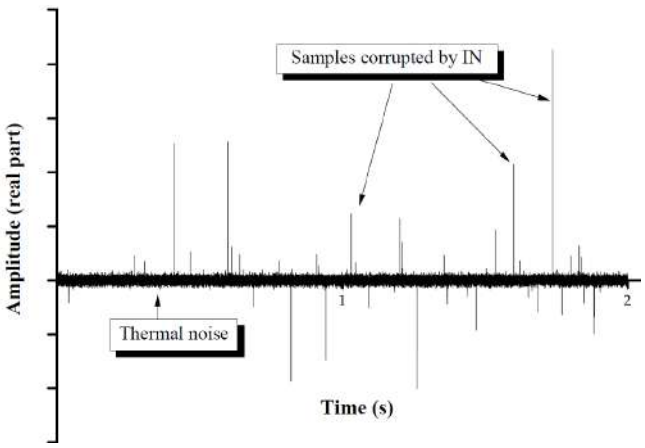

Figure 2. Impulsive noise plus thermal noise.

The pulse amplitude follows a log-normal distribution [16]. Therefore, to generate the values of the IN amplitudes, a Gaussian RV Z with mean A [dBμV] and standard deviation B [dB] is generated. Then, the value $Z = z$ [dBμV] is converted to its form $z[\mu V] = 10^{\frac{z[dB\mu V]}{20}}$.

The IN phase is modeled through an RV θ, with a uniform distribution between $(0, 2\pi]$. Thus, knowing the magnitude z and the phase θ of the IN samples, the in-phase and quadrature components of the IN can be expressed as $I = z\cos(\theta)$ and $Q = z\sin(\theta)$, respectively.

In real environments, not all samples will be contaminated with IN, but all will be affected by thermal noise. Fig. 2 illustrates an example of IN generated from the before-mentioned model, where the average pulse magnitude is $A = 70$ [dBμV], with a standard deviation of $B = 8.5$ [dB], and $\beta = 900$. The thermal noise power is 50 [dBμV], the sampling frequency is 30 kHz, and the total analysis time is two seconds, equivalent to 60000 samples.

To incorporate IN into the context of CSS, we consider creating three new parameters: i) K is the ratio between the average powers of IN and thermal noises $K = \sigma_{\mathrm{r}}^2/\sigma_{\mathrm{w}}^2$, where σ_{r}^2 is the variance of the IN; ii) P_{IN} is the probability of occurrence of IN during a sensing period, modeled as a Bernoulli RV; and iii) P_{CR} is the percentage of CRs affected by IN when it is present, modeled as a Binomial RV with parameters m and P_{CR}.

D. Primary User Signal in TV White Spaces

The PU signal considered in the SS simulations evaluated in this work is an OFDM-type signal, fully compliant with the ISDB-T/T$_{\mathrm{B}}$ (Integrated Services Digital Broadcasting - Terrestrial) TV standard, which is used in several countries, including Japan, Brazil, Argentina, and others, whose characteristics are detailed in the ABNT 15601 [17] standard and

Table I
OFDM ISDB-T_B SYSTEM TRANSMISSION PARAMETERS

Parameter	Value
Total number of carriers	8192 (Mode 3)
Number of active carriers	5617
Guard interval	1/16
Number of segments Layer A	13
Data carriers modulation Layer A	64-QAM
Encoding rate of layer A	7/8
Pilot carriers and TMCC modulation	BPSK/DBPSK
OFDM symbol duration	1.26 ms
Subcarrier spacing	0.992 kHz
Pilot spacing	11.9 kHz
IFFT clock	512/63 MHz
Bandwidth	5.572 MHz

can be mathematically described by

$$x(t) = \sum_{s=0}^{\infty} \sum_{k=0}^{K_T-1} c_{s,k}\psi(s,k,t), \tag{7}$$

where

$$\psi(s,k,t) = \begin{cases} e^{j2\pi \frac{k-K_c}{T_u}(t-T_g-sT_s)} & sT_s \leq t < (s+1)T_s \\ 0 & t < sT_s, t \geq (s+1)T_s \end{cases} \tag{8}$$

in which k is the index of the carrier, which is successive for the entire band, with the number 0 assigned to carrier 0 of segment 11; s is the symbol number; K_T represents the total carriers of the mode; T_s is the duration time of the OFDM symbol; T_g is the duration time of the guard interval; T_u is the duration time of the useful part of the symbol; f_c is the center frequency of the PU signal; K_c is the carrier number corresponding to the center frequency of the signal; and $c_{s,k}$ is the corresponding complex serial symbol to the OFDM symbol with index s and carrier index k.

III. DEVELOPMENTS OF SIMULATIONS

A. Generation of Primary User Signal in TVWS

Before starting the development of SS simulations with a focus on TVWS usage, an OFDM signal in compliance with the characteristics of a typical ISDB-T_B transmission signal was implemented in MATLAB. Table I presents the parameters used in implementing the OFDM signal, which will be incorporated into the SS simulations. The generated signal has a usable bandwidth of 5.57 MHz, as per the ISDB-T_B standard, as shown in Fig. 3, which displays the magnitude of power spectrum density of the generated OFDM signal. As expected by the standard, the entire signal is confined within the -3 MHz to 3 MHz bandwidth, with a minor guard band at the boundaries. The simulation did not convert the OFDM signal to channel frequency because, in practical SS, the first processing step is converting signals from channel frequency to baseband.

B. Final SS Simulation in TVWS

MATLAB software simulation has been developed to estimate SS's performance in a realistic TVWS scenario. The PU transmission signal, $x(t)$, is that presented in Subsection III-A; the channel gain, $h(t)$, is generated by random samples with a Rayleigh distribution with unit variance, representing a nLoS fading scenario between the CRs and PU; and the noise considered, $w(t)$, is the AWGN with zero mean and unitary variance. The IN, $r(t)$, is that described in Section II-C. The sampling frequency used in the simulation is set to match the IFFT clock value indicated in Table I, which ensures the detection of all signal power within a 6 MHz channel. The sensing technique considered is a cooperative version of ED (SF and DF), described in Section II-B. Therefore, the decision variable T_{ED}, used to define spectral occupancy, is calculated as presented in (2).

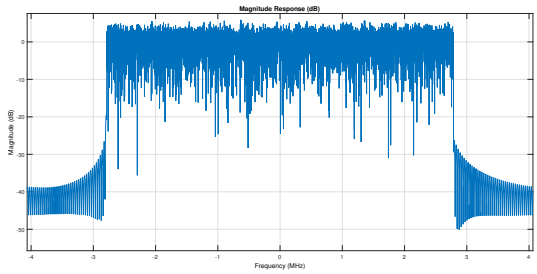

Figure 3. ISDB-T_B PU signal power spectrum density.

The simulation developed has as its main input parameters the number of CRs (m); the number of samples collected by each CR (n); the number of primary transmitters (p); the mean SNR; the number of Monte Carlo events of the simulation (N_e); the ratio between the IN power and the power of thermal noise present in the system (K); the probability of occurrence of the IN (P_{IN}); the average percentage of CRs affected by the IN (P_{CR}); the average spacing between IN samples (β); the mean value of the log-normal IN amplitudes (A); and the standard deviation of the log-normal IN amplitudes (B).

IV. NUMERICAL RESULTS

This section presents the performance results of SS in various TVWS scenarios using the receiver operating characteristic (ROC) curve and the area under the curve (AUC) metrics. All performance curves presented in this section were obtained through careful simulations developed on the MATLAB software platform, according to section III-B, which took into account 20000 Monte Carlo events (50% of the events are considered under the hypothesis $\mathcal{H}_0$ and 50% under hypothesis $\mathcal{H}_1$). The IN parameters, when present, are highlighted in the presented performance figures.

A. Cooperative Performance in the absence and presence of IN

To verify the performance of the CSS system in the presence and the absence of IN, simulations with the following parameterization have been carried out: $p = 1$, $n = 60$, $m = 6$, decision methods SF and DF, and SNR $= -8$ dB (with and without IN) and -15 dB (with IN). The resulting ROC curves and the AUC values obtained for each simulated case are

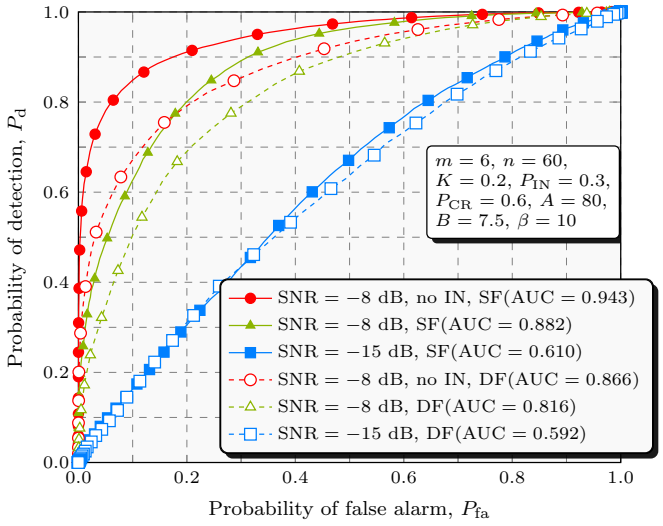

Figure 4. ROC curves in the presence and the absence of IN.

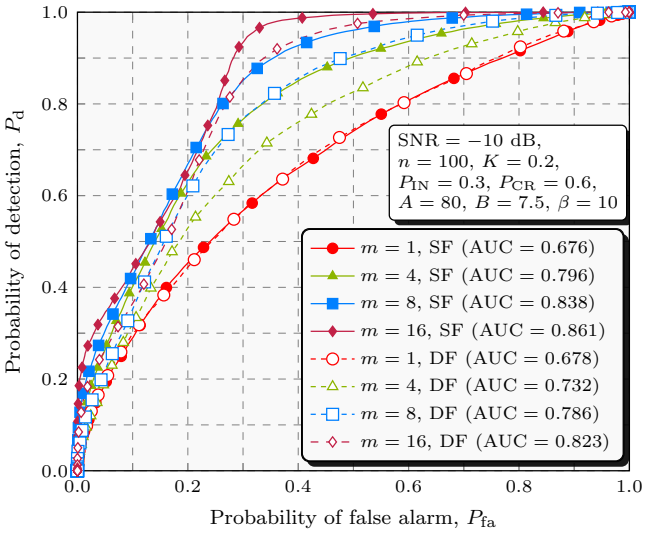

Figure 5. ROC curves under IN for different values of m.

presented in Fig. 4. The results shown in Fig. 4 indicate that the presence of IN reduces performance compared to the case without IN, regardless of the decision methods applied (SF or DF). This reduction is evident as the ROC curves move away from the optimal operating point ($P_d = 1$ and $P_{fa} = 0$), and the AUC metric decreases. Additionally, the SF method performs better than the DF in all evaluated cases. However, the performance reduction between the DF and SF appears to be less pronounced in scenarios with IN. For lower SNRs (SNR $= -15$ dB), the performance of the two techniques becomes quite similar.

B. Performance under IN for different numbers of CRs

To assess the influence of the number of CRs in a scenario with IN and compare its impact on CSS and non-CSS systems, a simulation has been performed with the following parameterization: $p = 1$, $n = 100$, SNR $= -10$ dB, decision methods SF and DF, and $m = \{1, 2, 4, 6, 8, 16\}$. Fig. 5 presents the ROC curves for each evaluated case. Fig. 5 shows that the cooperative approach offers notable advantages in mitigating IN compared to a non-CSS system ($m = 1$) for both SF and DF methods. However, as the number of CRs in the system increases, it is observed that performance gains tend to diminish, mainly considering low P_{fa} values. In other words, increasing the number of CRs does not significantly improve SS performance beyond a certain point. This conclusion could be crucial in defining the ideal number of CRs in the cooperative network, ensuring good performance without excessively raising the network cost associated with CR acquisition for sensing purposes. The results obtained with SF and DF for $m = 1$ are practically the same since, in both cases, the decision is based only on the samples of the single considered CR. For other values of m, the SF method performed better than the DF method for the considered level of IN. For example, for $m = 16$, the AUC metric for SF is 0.861, while for DF is 0.813.

C. Performance under different IN parameters

The impact of IN parameters (K, P_{IN}, P_{CR}, and β) [1] on the CSS have been evaluated. All simulations carried out in this subsection have been performed considering a Rayleigh channel and use the following fixed parameterization: $p = 1$, $n = 100$, $m = 6$, decision methods SF and DF, and SNR $= -10$ dB.

To evaluate the influence of IN intensity on the performance of the sensing system, simulations have been conducted using $K = \{0, 0.2, 2\}$. The resulting ROC curves and all simulation parameters are presented in Fig. 6 (a). It can be seen that increasing K results in a performance drop in SS because the IN increases the uncertainty in the FC's decision, which translates into an increase in the probability of false alarms. It is also observed that in the absence of IN ($K = 0$), the SF method (AUC $= 0.916$) outperforms the DF technique (AUC $= 0.838$). However, as K increases, this performance difference decreases, and for a significantly high K value ($K = 2$), the DF technique (AUC $= 0.714$) surpasses the SF technique (AUC $= 0.706$) despite its simpler practical implementation.

To interpret how the probability of occurrence of IN affects the performance of the SS system using both fusion methods, its value was varied in the simulation according to $P_{IN} = \{0, 0.2, 0.4\}$. Fig. 6 (b) presents the resulting ROC curves and detailed parameters. As expected, increasing P_{IN} reduces the performance of the sensing system using either of the fusion techniques. Once again, in the absence of IN ($P_{IN} = 0$), the SF technique outperforms the DF technique. However, as the IN occurrence probability increases, the DF technique

[1] It is worth mentioning that the IN parameters A and B were also varied in the simulations; however, they did not significantly affect the performance of SS. We conjecture this occurs due to the normalization of IN power by the K factor, which adjusts the IN power to be K times greater than that of thermal noise, regardless of the selected values of A and B.

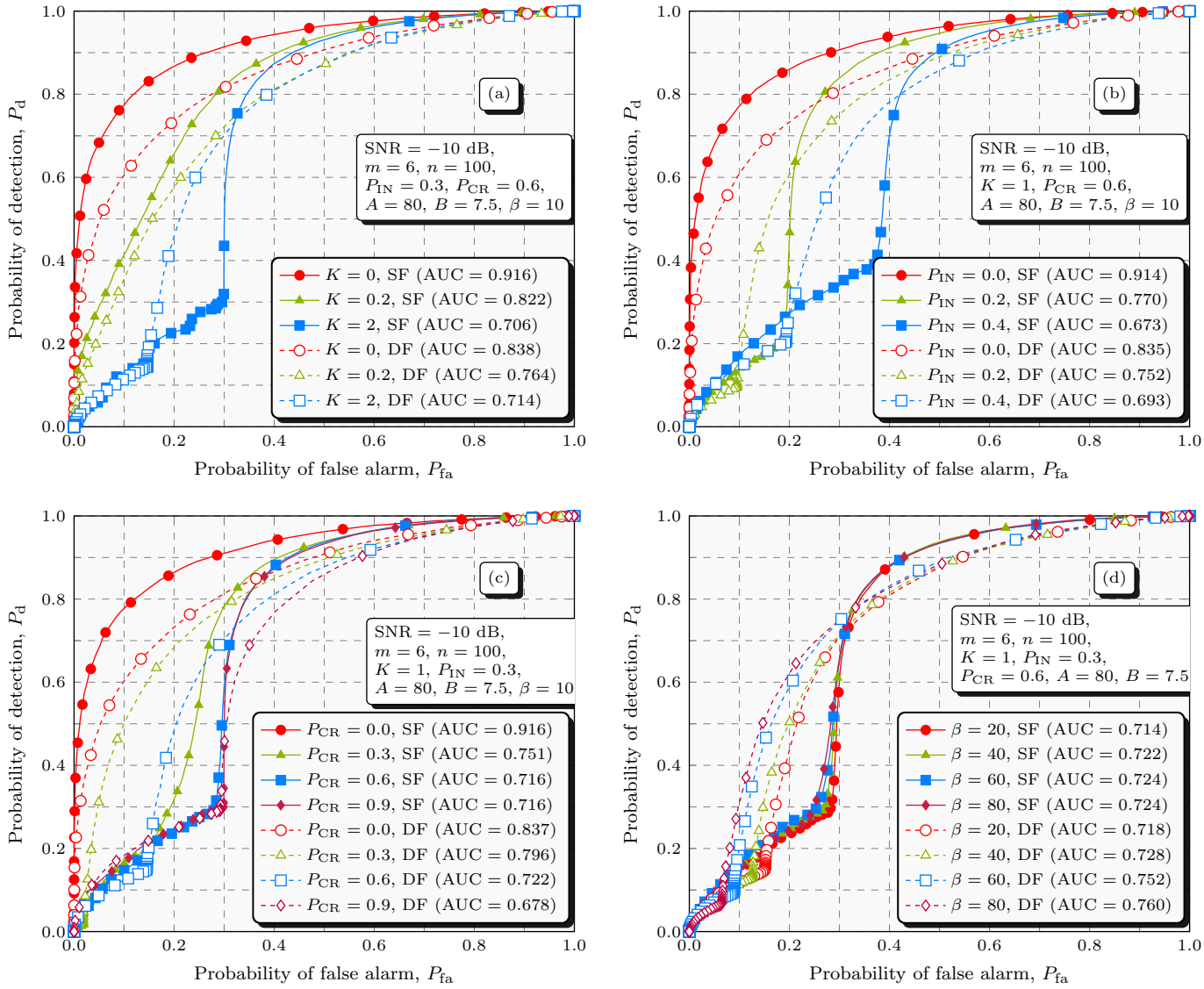

Figure 6. ROC curves for different values of K (a), P_{IN} (b), P_{CR} (c), and β (d).

performs better than the SF technique. The ROC curves for the SF technique exhibit interesting behavior when intense IN is present in the system, such as when $K = 1$ occurs. The ROC curves (solid blue and green) exhibit a sharp vertical drop near $P_{\text{fa}} = P_{\text{IN}}$, continuing to a point near $P_{\text{fa}} = P_{\text{d}} = P_{\text{IN}}$. This sharp vertical drop happens because when very intense IN is present, the probability of false alarm approaches the probability of detection for higher threshold values, indicating operational infeasibility under these conditions. On the other hand, while the DF technique also suffers degradation, it maintains superior performance with a smoother decline in the ROC curve. In particular, the DF technique's SS performance (AUC $= 0.693$) for $P_{\text{IN}} = 0.4$ surpasses that of the SF technique (AUC $= 0.673$).

To understand the impact of the percentage of CRs corrupted when IN is present, this parameter was varied in the simulation as follows: $P_{\text{CR}} = \{0, 0.3, 0.6, 0.9\}$. The resulting ROC curves and detailed information on the parameters used are presented in Fig. 6 (c). It is observed that an increase in P_{CR} leads to a reduction in system performance for both fusion techniques, as more collected samples processed at the CRs (for DF) or at the FC (for SF) are corrupted by IN. Another important conclusion that can be drawn from the analysis of Fig. 6 (c) is that in situations where IN is present ($P_{\text{CR}} \neq 0$), the lower the percentage of affected CRS, the better the performance of the DF technique compared to the SF method. For example, for $P_{\text{CR}} = 0.3$, the AUC for SF is 0.751, whereas for DF it is 0.796. This performance improvement can be justified by the fact that in high-intensity IN situations (such as the used $K = 1$), regardless of the number of CRs affected, sensing is already compromised in the SF method since all samples are considered for computing the final cooperative decision variable T_{ED}. In contrast, in the DF technique, since

the decision on occupancy is made in favor of the majority of individual decisions, if only a few CRs are corrupted by intense IN, the decisions of the unaffected CRs can still lead to an accurate SS decision.

Finally, the average distance between IN samples was varied in the simulation according to $\beta = \{20, 40, 60, 80, 100\}$, and the ROC curves are presented in Fig. 6 (d) along with the other systemic parameters considered. By inspection of results, it is possible to observe that the increase in β improves system performance using both fusion techniques, which is justifiable since, with the increase in the spacing between IN samples, the effective number of IN pulses inserted into the samples captured by the cooperative network's CRs is reduced. It is also observed that the set of curves generated in the simulation using the SF method (solid curves) shows a significant performance degradation for $P_{\text{fa}} \approx 0.3$. In contrast, the group of curves employing the DF technique achieves a smoother decline in the ROC curves and a higher detection probability for $0.1 < P_{\text{fa}} < 0.3$. In all cases evaluated in Fig. 6 (d), the DF technique provided a higher AUC value than that achieved by the SF technique. The aforementioned improvement demonstrates that although the DF technique is simpler to implement due to not requiring the transmission of all samples collected by the CRs in the cooperative network to the CF, in several cases of intense external interference, the DF technique provides superior performance compared to that achieved by the SF fusion method, making it the more suitable choice for this type of environment.

V. Conclusions

This work has advanced the study of CSS in TVWS scenarios using two distinct cooperation methods: SF and DF. Our study specifically has addressed a practical PU signal, the ISDB-T$_B$, under realistic disturbances such as Rayleigh fading in the received signal, thermal noise, and IN. The analyses have enabled a comprehensive comparison of several scenarios, demonstrating the negative impact of IN on SS performance. Additionally, it has been observed that increasing the number of CRs leads to performance improvements, although these gains diminish as the number of CRs increases. We also have evaluated the impact of various IN parameters on SS. Significant and non-obvious conclusions have been drawn regarding the two considered fusion methods. It has been found that in several situations, mainly those with high IN power intensity but a low percentage of affected CRs, the DF technique outperforms the SF technique despite its lower implementation complexity. These understandings are critical for optimizing SS strategies, helping to enhance the robustness and reliability of CSS in TVWS.

References

[1] H. B. Sandya, K. Nagamani, and L. Shavanthi, "A review of cognitive radio spectrum sensing methods in communication networks," in *2018 International Conference on Communication and Signal Processing (ICCSP)*, 2018, pp. 0457–0461.

[2] "Resolução ANATEL Nº 747," Conselho diretor Anatel, 10/2021, 2021, Access in June 2024. [Online]. Available: https://www.gov.br/anatel/pt-br/assuntos/noticias/anatel-publica-resolucao-para-uso-de-espectro-ocioso

[3] M. Ali, M. N. Yasir, D. M. S. Bhatti, and H. Nam, "Optimization of spectrum utilization efficiency in cognitive radio networks," *IEEE Wirel. Commun. Lett.*, vol. 12, no. 3, pp. 426–430, 2023.

[4] V. Amrutha and K. V. Karthikeyan, "Spectrum sensing methodologies in cognitive radio networks: A survey," in *2017 International Conference on Innovations in Electrical, Electronics, Instrumentation and Media Technology (ICEEIMT)*, 2017, pp. 306–310.

[5] X. Liu, M. Jia, M. Zhou, B. Wang, and T. S. Durrani, "Integrated cooperative spectrum sensing and access control for cognitive industrial internet of things," *IEEE Internet Things J.*, vol. 10, no. 3, pp. 1887–1896, 2023.

[6] K. Captain, A. Chauhan, and R. Kumar, "Channel coding for cooperative spectrum sensing under imperfect reporting channels," in *2022 14th International Conference on COMmunication Systems & NETworkS (COMSNETS)*, 2022, pp. 482–487.

[7] D. Janu, S. Kumar, and K. Singh, "A graph convolution network based adaptive cooperative spectrum sensing in cognitive radio network," *IEEE Trans. Veh. Technol.*, vol. 72, no. 2, pp. 2269–2279, 2023.

[8] M. Oner and F. Jondral, "Cyclostationarity based air interface recognition for software radio systems," in *Proceedings. 2004 IEEE Radio and Wireless Conference (IEEE Cat. No.04TH8746)*, 2004, pp. 263–266.

[9] Y. Zeng, Y.-C. Liang, A. T. Hoang, R. Zhang, and Z. Liu, "A review on spectrum sensing for cognitive radio: Challenges and solutions," *EURASIP Journal on Advances in Signal Processing*, 2010.

[10] W. Zhao, H. Li, M. Jin, Y. Liu, and S.-J. Yoo, "Eigenvalues-based universal spectrum sensing algorithm in cognitive radio networks," *IEEE Syst. J.*, vol. 15, no. 3, pp. 3391–3402, 2021.

[11] Y. Arjoune and N. Kaabouch, "A comprehensive survey on spectrum sensing in cognitive radio networks: Recent advances, new challenges, and future research directions," *Sensors*, vol. 19, no. 1, 2019.

[12] H. Huang and C. Yuan, "Cooperative spectrum sensing over generalized fading channels based on energy detection," *China Communications*, vol. 15, no. 5, pp. 128–137, 2018.

[13] W. Wu, Z. Wang, L. Yuan, F. Zhou, F. Lang, B. Wang, and Q. Wu, "Irs-enhanced energy detection for spectrum sensing in cognitive radio networks," *IEEE Wirel. Commun. Lett.*, vol. 10, no. 10, pp. 2254–2258, 2021.

[14] C. Vlădeanu, A. Marţian, and D. C. Popescu, "Spectrum sensing with energy detection in multiple alternating time slots," *IEEE Access*, vol. 10, pp. 38 565–38 574, 2022.

[15] D. M. M. Plata and Á. G. A. Reátiga, "Evaluation of energy detection for spectrum sensing based on the dynamic selection of detection-threshold," *Procedia Engineering*, vol. 35, pp. 135–143, 2012.

[16] P. Torío and M. García Sánchez, "Generating impulsive noise [wireless corner]," *IEEE Antennas Propag. Mag.*, vol. 52, no. 4, pp. 168–173, 2010.

[17] "Televisão digital terrestre - Sistema de transmissão," Associação Brasileira de Normas Técnicas - ABNT 15601, Rio de Janeiro, 2007, Access in November 2022. [Online]. Available: https://www.normas.com.br/visualizar/abnt-nbr-nm/26689/nbr15601-televisao-digital-terrestre-sistema-de-transmissao